Energy Engineering

Tech Science Press

DOI: 10.32604/ee.2023.028620

ARTICLE

Parameters Identification for Extended Debye Model of XLPE Cables Based on Sparsity-Promoting Dynamic Mode Decomposition Method

Weijun Wang[1,*], Min Chen[1], Hui Yin[1] and Yuan Li[2]

[1]Guiyang Power Supply Bureau, Guizhou Power Grid Co., Ltd., Guiyang, 550004, China

[2]College of Electrical Engineering, Sichuan University, Chengdu, 610065, China

[*]Corresponding Author: Weijun Wang. Email: gnosis666@163.com

Received: 22 December 2022 Accepted: 10 March 2023 Published: 28 September 2023

ABSTRACT

To identify the parameters of the extended Debye model of XLPE cables, and therefore evaluate the insulation performance of the samples, the sparsity-promoting dynamic mode decomposition (SPDMD) method was introduced, as well the basics and processes of its application were explained. The amplitude vector based on polarization current was first calculated. Based on the non-zero elements of the vector, the number of branches and parameters including the coefficients and time constants of each branch of the extended Debye model were derived. Further research on parameter identification of XLPE cables at different aging stages based on the SPDMD method was carried out to verify the practicability of the method. Compared with the traditional differential method, the simulation and experiment indicated that the SPDMD method can effectively avoid problems such as the relaxation peak being unobvious, and possessing more accuracy during the parameter identification. And due to the polarization current being less affected by the measurement noise than the depolarization current, the SPDMD identification results based on the polarization current spectral line proved to be better at reflecting the response characteristics of the dielectric. In addition, the time domain polarization current test results can be converted into the frequency domain, and then used to obtain the dielectric loss factor spectrum of the insulation. The integral of the dielectric loss factor on a frequency domain can effectively evaluate the insulation condition of the XLPE cable.

KEYWORDS

Cable insulation; dielectric response; sparsity-promoting dynamic mode decomposition; parameter identification

1 Introduction

Cross-linked polyethylene (XLPE) cable has become the core transmission equipment in urban distribution networks because of its excellent electrical and mechanical properties, simple installation, large transmission capacity and other advantages [1]. However, during the long-term operation, the insulation performance of XLPE cables will deteriorate gradually due to the combined effects of electrical, thermal, moisture and mechanical stresses. Therefore, the rapid and effective diagnosis of the cable insulation state can provide a guarantee for the safe and stable operation of the power system. In recent years, dielectric response technology has attracted more and more attention as a non-destructive test method on insulating materials. The polarization and depolarization current (PDC) measurement in time-domain is especially suitable for the on-field diagnosis of high-voltage electrical equipment because of its fast, accurate, and abundant test information [2–6].

The extended Debye model is an abstract model based on the dielectric response theory, with consideration of the relaxation and conductance process inside the dielectric. The model has clear physical concept and concise model parameters. With the help of this model, the details of dielectric measurements such as PDC can be well explained and analyzed [6–8]. As per the assessment of the dielectric status using the extended Debye model, accurate and unique identification of the model parameters is a prerequisite. The traditional method to derive the model parameters is mainly by fitting, that is, the mathematical expression of polarization/depolarization current is first listed according to the Debye equivalent circuit with a preset fixed number of branches, and then the model parameters are obtained by fitting the current curve according to the formula [9]. With the development of intelligent algorithms, various optimization algorithms are used to improve the accuracy of the identification of the extended Debye model parameters. References [8,10] introduced the cuckoo search algorithm and gray wolf optimization algorithm for parameter identification of the extended Debye model, respectively. However, intelligent algorithms have some natural shortcomings, such as slow convergence speed and being easy to fall into local optimal solution, which leads to a non-unique parameter identification result. In addition, fitting methods essentially take the established model as the research object, that is, the number of relaxation branches of the extended Debye model needs to be set artificially according to relevant experience or theoretical support. However, for the dielectric with ambiguous relaxation mechanism, the number of relaxation branches is always difficult to determine. In order to solve this problem, references [11,12] preseted multiple equivalent circuits with different numbers of branches, and use the fitting method to process them respectively, and finally select the multi-branch equivalent circuit model with the highest fitting goodness as the identification result. However, this kind of heuristic processing method requires manual modification of algorithm parameters for many times, which is inefficient. In addition, manually setting branches without actual relaxation processes loses the physical meaning of the extended Debye model.

For this reason, reference [6] first determined the number of branches of the model by using the piecewise analytical method, and the depolarization current differential method combined with the current spectral line characteristics, respectively, and then further solves the model parameters on this basis. Although the above methods take the determination of the number of model branches into account, subsequent studies have shown that the identification accuracy is greatly affected when the time constant distribution of the medium relaxation process is close [13]. In addition, the identification accuracy of the above methods is easily affected by the measurement noise.

In addition, all the above methods take the depolarization current spectral line as the original data, without considering the use of the measured polarization current results. The advantages of using polarization current to identify parameters are as follows: *i*. According to the basic principle of PDC test, if the model parameters can be identified only by polarization current spectral lines, the test time can be halved, and the power outage time of the field test can be greatly reduced. The research results of reference [14] showed that the dielectric response analysis and parameter calculation results using only polarization current and using polarization/depolarization current at the same time are consistent, which verifies the rationality and effectiveness of polarization current as the original data. *ii*. The influence of noise on the test results and identification results of polarization current is relatively small [15]. The specific reason is that the polarization current contains a steady-state DC conduction current component, and the existence of DC bias makes the measured amplitude larger than that of the depolarization current, thus possessing a stronger anti-noise capability.

In order to solve the above problems, the extended Debye model of XLPE cable based on the polarization current characteristics is first introduced in this paper. Afterwards, the sparsity-promoting dynamic mode decomposition (SPDMD) method is introduced to realize the identification of model parameters, while meeting the requirements of clear physical meaning and mathematical fitting goodness at the same time. The advantages and rationality of adopting the polarization current spectral lines as the analytic object of the model are discussed in detail. Finally, the effectiveness of the proposed method is verified by the practical application of the method to XLPE cable samples with different thermal aging statuses.

2 Extended Debye Model of XLPE Cables

The extended Debye model of the dielectric is represented by a multi-branch *R*-*C* equivalent circuit composed of a series of resistors and capacitors, as shown in Fig. 1. Each branch of the *R*-*C* equivalent circuit represents the relaxation process of the dielectric [16]. In the polarization stage of the PDC test, R_0 represents the steady-state conductance process of the dielectric under the influence of the applied electric field; C_0 is the geometric capacitance of the measured dielectric, which represents the sum of the instantaneous polarization process in the dielectric. The frequency band of this response process is much higher than the acquisition frequency of the measuring equipment, so it cannot be recorded in the actual measurement process; R_i, $C_i (i = 1, 2, \ldots, n)$ series branches represent various relaxation processes of the medium under the electric field, which are independent of each other and have different relaxation times $\tau_i = R_i C_i$. To sum up, the polarization current of the PDC test can be expressed as

$$i_p = A_0 + \sum_{i=1}^{n} A_i e^{-t/\tau_i} \tag{1}$$

where, A_0 is the steady-state conductance current of R_0 branch; A_i is the relaxation intensity coefficient of the ith *R*-*C* series branch; *t* is the polarization time, and *n* is the number of series branches, i.e., the number of relaxation processes with different mechanisms in the dielectric.

Further have

$$R_0 = U_0/A_0 \tag{2}$$

$$R_i = U_0/A_i \tag{3}$$

$$C_i = t_i/R_i \tag{4}$$

where U_0 is the applied polarization voltage.

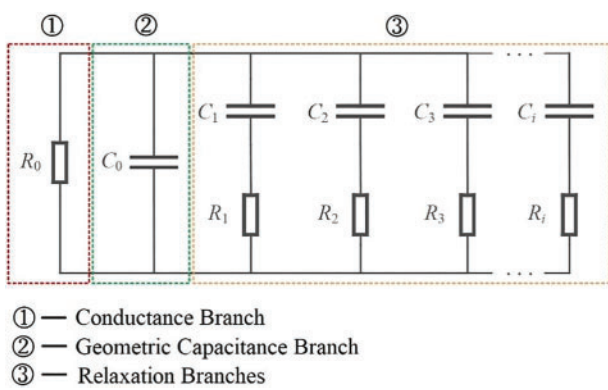

Figure 1: Extended Debye equivalent circuit model

To sum up, to identify the extended Debye model parameters, it is necessary to determine the number n of relaxation branches of the model, and then obtain the steady-state conductance current value A_0, the relaxation intensity coefficient A_i of each branch, and the relaxation time τ_1.

3 Parameter Identification Based on SPDMD Method

Based on the characteristics of the extended Debye model and the PDC test current signal, the performance of the commonly used dominant modal parameter identification method is comprehensively analyzed. It is found that the identification results of the Prony algorithm are greatly affected by the measurement noise [17], and the TLS-ESPRIT algorithm has a large demand for computing power consumption due to the existence of two singular value decompositions [18]. The matrix pencil algorithm and the random subspace algorithm also have the disadvantage that the order of the model is difficult to be uniquely determined. The SPDMD method extracts the dominant mode according to the spatiotemporal evolution law of the test signal, and comprehensively considers the influence of noise interference and computational complexity. Therefore, it has its unique advantages in the identification of the dielectric parameters of the Debye model of polarization current [19].

3.1 Mode Decomposition of Polarization Current Signal Based on DMD Algorithm

Firstly, the polarization current sampling signal $X(i)(i = 1, 2, \ldots, N)$ is adopted to build a Hankel matrix as the following:

$$\boldsymbol{X} = \begin{bmatrix} x(1) & x(2) & \cdots & x(L) \\ x(2) & x(3) & \cdots & x(L+1) \\ \vdots & \vdots & \vdots & \vdots \\ x(N-L+1) & x(N-L+2) & \cdots & x(N) \end{bmatrix} \tag{5}$$

Let $X = [x_1, x_2, \ldots, x_L]$. The former $(L-1)$ column vectors and the latter $(L-1)$ column vectors of the matrix X are extracted respectively to construct matrix $X_1 = [x_1, x_2, \ldots, x_{L-1}]$, and matrix $X_2 = [x_2, x_3, \ldots, x_L]$. According to the basic principle of DMD, the two matrices have the following relationship,

$$\boldsymbol{X}_2 = \boldsymbol{A}\boldsymbol{X}_1 \tag{6}$$

where, A is a high-order mapping matrix that records the dynamic change characteristics of the sampling signal sequence, and a low-order matrix F can be introduced to approximately describe A to reduce the amount of calculation. F can be expressed as

$$\boldsymbol{F} = \boldsymbol{U}^*\boldsymbol{A}\boldsymbol{U} \tag{7}$$

where U is the left singular vector matrix of the matrix X_1 subjected to singular value decomposition as shown in the following formula:

$$\boldsymbol{X}_1 = \boldsymbol{U}\boldsymbol{\Sigma}\boldsymbol{V}^* \tag{8}$$

F can be obtained by calculating the Eqs. (6)–(8). Afterwards, perform the eigenvalue decomposition on matrix F,

$$\boldsymbol{F} = \boldsymbol{U}^*\boldsymbol{X}_2\boldsymbol{V}\boldsymbol{\Sigma}^{-1} = \boldsymbol{Y}\boldsymbol{\Lambda}\boldsymbol{Y}^{-1} \tag{9}$$

where $\Lambda = [l_1, l_2, \ldots, l_N]$ is the eigenvalue matrix, $l_i(i = 1, 2, \ldots, n)$ are non-zero eigenvalue, and n is the number of branches obtained by identification.

3.2 SPDMD Algorithm

When the traditional DMD method is used to identify the Debye model parameters of the measured PDC signal, the existence of measurement noise will make the zero eigenvalue in the eigenvalue matrix Λ in Eq. (9) become non-zero, which will lead to the misjudgment of the model order, and the introduction of false modes. Therefore, the determination of true modal order is one of the core steps of modal identification. In this paper, the current flowing through the relaxation and conductance branches of Debye's equivalent circuit model in the PDC test signal is the true mode. In this section, SPDMD is introduced to distinguish it from spurious modes, so as to determine the number of Debye model branches.

First, the Vandermonde matrix V_{and} is constructed,

$$\boldsymbol{V}_{\text{and}} = \begin{bmatrix} 1 & \lambda_1 & \cdots & {\lambda_1}^{N-1} \\ 1 & \lambda_2 & \cdots & {\lambda_2}^{N-1} \\ \vdots & \vdots & \vdots & \vdots \\ 1 & \lambda_n & \cdots & {\lambda_n}^{N-1} \end{bmatrix} \tag{10}$$

Through the optimized solution of the signal DMD mode amplitude [16], the amplitude vector shown below can be finally obtained as $a = [a_1, a_2, \ldots, a_N]^T$, where $a_i (i = 1, 2, \ldots, n)$ is the modal amplitude coefficient.

$$\boldsymbol{\alpha} = \left((\boldsymbol{Y}^* \boldsymbol{Y}) \circ (\overline{\boldsymbol{V}_{\text{and}} {\boldsymbol{V}_{\text{and}}}^*}) \right)^{-1} \overline{\text{diag}(\boldsymbol{V}_{\text{and}} \boldsymbol{V} \boldsymbol{\Sigma}^* \boldsymbol{Y})} \tag{11}$$

In this formula, o represents the multiplication of the elements at the corresponding positions in the two matrices, and the overline represents the complex conjugation of a matrix or vector.

After obtaining the DMD modal, amplitude vector α of the signal can be derived. The enhanced sparse amplitude vector α_{Sp} can be further obtained by introducing the sparsity penalty function to highlight the real mode of the model. The solution result of the enhanced sparse amplitude vector is expressed as follows:

$$\boldsymbol{\alpha}_{\text{sp}} = [\boldsymbol{I} \quad \boldsymbol{0}] \begin{bmatrix} \boldsymbol{P} & \boldsymbol{E} \\ \boldsymbol{E}^T & \boldsymbol{0} \end{bmatrix}^{-1} \begin{bmatrix} \boldsymbol{q} \\ \boldsymbol{0} \end{bmatrix} \tag{12}$$

where I is the identity matrix. $\boldsymbol{P} = \left((Y^* Y) \circ (\overline{\boldsymbol{V}_{\text{and}} {\boldsymbol{V}_{\text{and}}}^*}) \right)$, $\boldsymbol{q} = \overline{\text{diag}(\boldsymbol{V}_{\text{and}} \boldsymbol{V} \boldsymbol{\Sigma}^* \boldsymbol{Y})}$. E is the sparsity encoding matrix of the amplitude vector α. Each column of E is a unit vector, and the nonzero elements in E correspond to DMD modes with zero amplitude within α, for example, assuming $a = [a_1, 0, a_3, 0]^T$, then,

$$\boldsymbol{E} = \begin{bmatrix} 0 & 1 & 0 & 0 \\ 0 & 0 & 0 & 1 \end{bmatrix}^T \tag{13}$$

Through the construction of the enhanced sparse amplitude vector, the problems of screening the dominant mode of the model and eliminating the false mode introduced by noise are solved. In amplitude vector α, each element corresponds to the modal amplitude of each branch of the extended Debye model. Through enhancing the sparsity of vector α by the SPDMD algorithm, the signal contribution degree corresponding to the elements representing the dominant modal amplitude is further highlighted. Finally, it can be concluded that in the enhanced sparse amplitude vector α_{Sp}, the modes corresponding to the non-zero elements are the dominant modes, and the number of non-zero elements is the number of branches identified by the extended Debye model.

3.3 Parameter Identifying Process

When the above algorithm is used to identify the parameters of the Debye model derived from the polarization current, it can be seen from Eq. (1) that the steady-state conductance current A_0 can be equivalent to the current of the relaxation branch with a maximum decay time, that is, the Eq. (1) can be unified as the following:

$$i_\mathrm{p} = \sum_{i=0}^{n} A_i e^{-t/\tau_i} \tag{14}$$

In Eq. (14), τ_0 is the relaxation time constant of the DC conductance current, which tends to be infinite in theory. In the actual analysis of the computer program, if the relaxation time constant of a branch identified from the output result is much greater than the polarization test time, the branch is regarded as the steady-state conductance branch.

The Debye model parameter A_i and τ_i can be calculated from the eigenvalues in the matrix Λ described above.

$$\tau_i = -\frac{T_s}{\ln(\lambda_i)} \tag{15}$$

$$\begin{bmatrix} x(1) \\ x(2) \\ \vdots \\ x(N) \end{bmatrix} = \begin{bmatrix} 1 & 1 & \cdots & 1 \\ \lambda_1 & \lambda_2 & \cdots & \lambda_i \\ \vdots & \vdots & \vdots & \vdots \\ \lambda_1^{N-1} & \lambda_2^{N-1} & \cdots & \lambda_i^{N-1} \end{bmatrix} \begin{bmatrix} A_1 \\ A_2 \\ \vdots \\ A_N \end{bmatrix} \tag{16}$$

where T_s is the sampling interval of the PDC. The position of the non-zero element in α_Sp is then obtained, which determines the dominant modal parameter.

To sum up, the steps of the extended Debye model parameter identification based on the polarization current are summarized as follows:

i. measuring the polarization current signal, recording the amplitude of the applied polarization voltage and the sampling frequency, and then constructing a Hankel standardized matrix X as shown in Eq. (5).

ii. calculating the matrix F according to Eqs. (6)–(8), and performing eigenvalue decomposition on matrix F to obtain an eigenvalue matrix Λ.

iii. constructing a Vandermonde matrix V_and, solving to obtain the amplitude vector α of the DMD mode, and carrying out sparse processing and optimizing to get the enhanced sparse amplitude vector α_Sp that is capable of reflecting the dominant mode in the signal.

iv. calculating the parameters of the Debye model by using the Eqs. (15) and (16). It should be noted that the steady-state DC conductance is solved as a dielectric relaxation process, and its decay time constant is very large.

4 Simulation Results and Analysis

4.1 Feasibility Verification

With the help of the mathematical model of polarization current given by Eq. (1), a group of polarization current signals with three relaxation branches are simulated. The parameter settings are shown in Table 1. The branch with a coefficient of 0 is the steady-state DC branch. The polarization time is set to 1000 s, and the sampling frequency is 1.2 Hz, which is consistent with the parameters of the measured PDC described later. Fig. 2 shows the simulated polarization current waveform.

Table 1: Extended Debye model parameters of simulated polarization current

Relaxation branch term	Amplitude A_i/pA	Time constant $\tau_{i/s}$
0	80.0	/
1	600.0	6.40
2	260.0	54.98
3	69.0	500.25

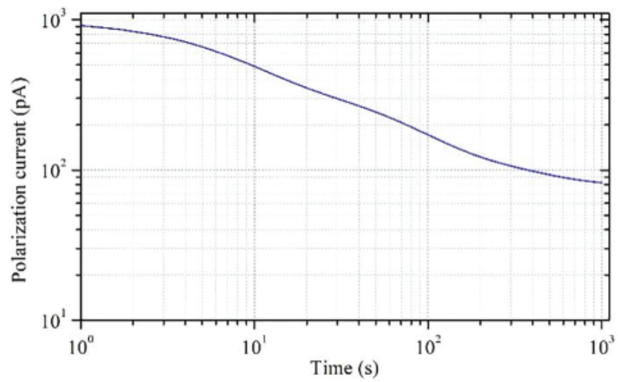

Figure 2: Simulated polarization current

Fig. 3 shows the vector α_{Sp} obtained by the SPDMD algorithm, where most of the elements are zero due to the sparsification. Some of the zero vector values are omitted in the figure. It can be clearly seen from the figure that the polarization current is composed of four relaxation modes (including DC component). Table 2 shows the parameter identification results corresponding to the four modes. The identification parameters are basically consistent with the pre-set parameters, indicating that the SPDMD method can well adapt to the determination of the number of branches and parameters of the Debye model.

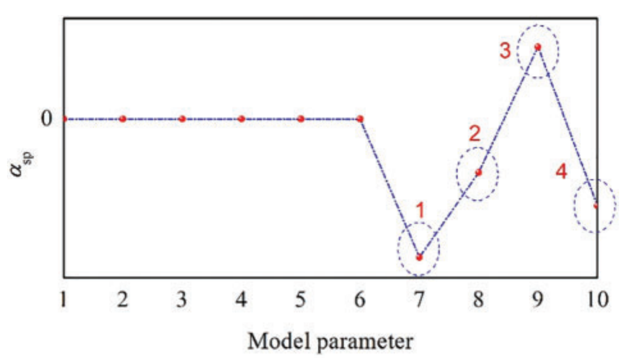

Figure 3: Sparsity-promoting amplitude vector results

In order to illustrate the superiority of the SPDMD method in determining the order of the number of branches of the Debye model, Fig. 4 shows the identification results of the polarization current curve shown in Fig. 2 by using the traditional differential method.

Table 2: Identification parameters of simulated polarization current

Relaxation branch term	Amplitude A_i/pA	Time constant $\tau_{i/s}$
0	80.0	2.21 × 1014
1	600.0	6.39
2	260.0	54.93
3	69.0	499.93

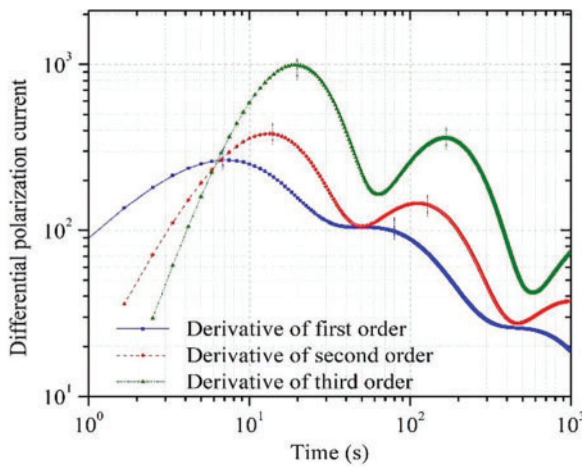

Figure 4: Identification result of simulated polarization current based on differential method

It can be seen from Fig. 4 that although there are three types of differential spectral lines, only two relaxation peaks can be distinguished, proving that the identification effect is not good. Through further analysis of the principle of the traditional differential method, its identification characteristics can be summarized as follows: the first derivative spectral line is prone to the superposition effect of relaxation peaks, which leads to the coverage of the peak points. Although the peak position can be effectively highlighted by increasing the differential order to reduce the half-peak width, it is achieved on the basis of sacrificing the maximum time constant of identification. Specifically, the maximum time constant value that can be effectively identified by the second derivative is 1/2 of the test time of PDC polarization/depolarization current, and the percentage of the third derivative is 1/3. Therefore, when there are relaxation processes with similar time constant or large time constant, there will be a blind area of identification by using traditional differential method. The SPDMD method introduced in this paper overcomes the above drawbacks in the application process.

4.2 Analysis of Anti-Noise Performance

The existence of the measurement noise is an unavoidable problem in the PDC test process, especially in substations with complex electromagnetic environments and dense distribution of buses and feeders [20]. Therefore, it is necessary to evaluate the anti-noise performance of the proposed PDC data analysis. In this section, Gaussian white noise with different intensities is added to the simulated polarized current signal, and then the parameters of the noised current signal are identified. Since the PDC current spectral line shows an exponential decay trend as a whole, the environmental noise mainly has a greater impact on the low amplitude period at the end of the signal. Therefore, the noise level η in this section is defined as the ratio of the standard deviation σ_{noise} of the noise to the current amplitude at the end of the polarization current,

$$\eta = \frac{\sigma_{\text{noise}}}{x(N)} \tag{17}$$

The determination coefficient R^2 is introduced to further quantify the identification effect under noise interference. This value reflects the goodness of fit of the model to the original data. The specific calculation formula is shown below. The closer the value is to 1, the higher the goodness of fit is.

$$R^2 = 1 - \frac{\sum_{i=1}^{N} \left| X(i) - \hat{X}(i) \right|^2}{\sum_{i=1}^{N} \left| X(i) - \frac{1}{N} \sum_{i=1}^{N} \hat{X}(i) \right|^2} \tag{18}$$

where $X(i)$ is the measured data. $\hat{X}(i)$ is the fitting data.

Afterwards, 200 times of Monte Carlo simulations are carried out for each group of noisy polarization current signals to exclude the influence of accidental factors. Table 3 shows the identification results of the extended Debye model parameters of the polarization current under the interference of different noise levels. It should be noted that the results are the average values of 200 times of simulation. Fig. 5 shows the polarization current spectral lines established according to the parameters in the table. It can be seen that the method in this paper has an excellent effect on the identification of polarization current under the condition of low noise, and only when the noise intensity is above 5%, the identification parameters of the large time constant branch will be significantly affected.

Table 3: Identification parameters of simulated polarization current under noisy conditions

η	A_0	τ_0	A_1	τ_1	A_2	τ_2	A_3	τ_3	R^2
0.5%	80.83	9.56×10^4	599.85	6.40	259.80	54.76	67.49	502.19	1.0000
1%	81.01	1.11×10^5	600.40	6.38	260.34	54.95	67.81	496.92	0.9998
3%	82.54	5.73×10^4	597.62	6.35	251.26	52.56	65.68	535.70	0.9983
5%	75.60	2.80×10^4	603.71	6.46	224.55	50.15	77.66	404.83	0.9823

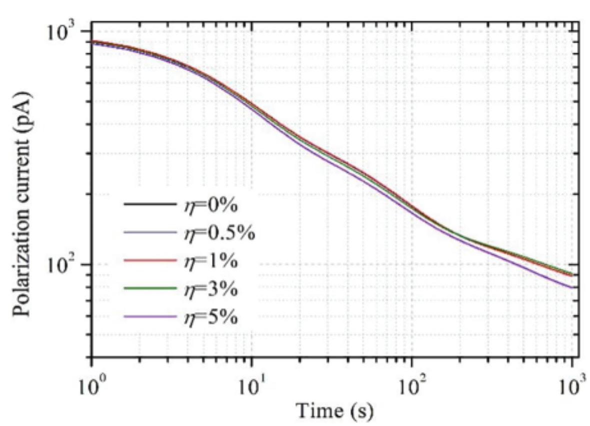

Figure 5: Identified polarization current curve under noisy conditions

5 Example Validations

5.1 Parameter Identification of Cables at Different Aging Stages

In order to test the effect of the proposed SPDMD method in the identification of dielectric parameters of actual power cables, the YJLV22-8.7/15 kV XLPE cable produced by Sunway Co., Ltd., China is selected as the experimental object. Firstly, several short cable samples with a length of 50 cm are made and put into the temperature and humidity control tank for thermal aging. The aging temperature and the relative humidity are set to 135°C and 0%, respectively. The samples are taken periodically from the tank and measured with PDC method, upon which the parameters of the cables are identified. PDC test platform is shown in Fig. 6. The test time is set to 1000 s. The sampling frequency is 1.2 Hz, and the test voltage is 1 kV.

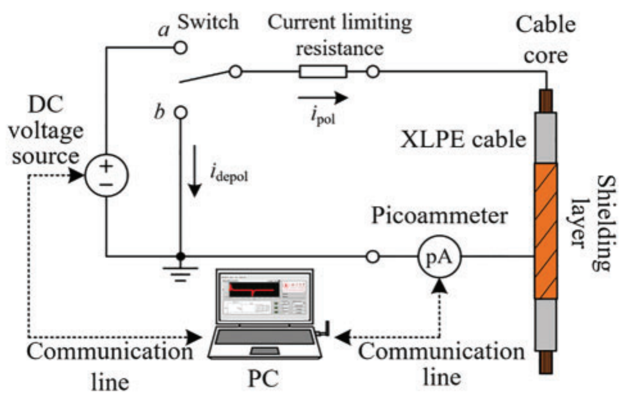

Figure 6: Diagram of the PDC measurement

In this section, the SPDMD method is used to identify the parameters of the extended Debye model derived from the polarization current of the new cable sample, the sample thermally aged for 15 days and the sample thermally aged for 30 days. The results are shown in Tables 4–6, respectively. Based on the value of the enhanced sparse amplitude vector α_{sp}, the number of relaxation branches of the cable's extended Debye model has increased from four branches before aging to five branches after aging, which indicates that a new relaxation process has occurred during the thermal degradation of the cable insulation. Also, the results indicate that the fitting method may make the parameter identification fall into an ill-conditioned state due to the lack of steps to determine the number of model branches. Fig. 7 shows the comparison of the polarization current curves drawn from the identification parameters and the actual measured, where the calculated fitting coefficients R^2 are 0.9993, 0.9996 and 0.9990, respectively. The results prove the superiority of the SPDMD method. Besides, we also adopt the SPDMD method on the depolarization current of PDC test to identify the parameters of the Debye model. The fitting coefficient R^2 are 0.9316, 0.9143 and 0.8971, respectively, indicating that the SPDMD method is more accurate when being adopted to the polarization current rather than the depolarization current of PDC test.

Table 4: Identification parameters of unaged samples

Relaxation branch term	Amplitude A_i/pA	Time constant $\tau_{i/s}$
0	116.0	3.25×10^5
1	2610.2	1.48

(Continued)

Table 4 (continued)

Relaxation branch term	Amplitude A_i/pA	Time constant $\tau_{i/s}$
2	177.6	2.34
3	160.4	9.58
4	40.6	49.84

Table 5: Identification parameters of 15 d aged samples

Relaxation branch term	Amplitude A_i/pA	Time constant $\tau_{i/s}$
0	243.0	5.76×10^5
1	2580.0	3.13
2	2220.3	36.89
3	180.6	49.59
4	107.9	136.31

Table 6: Identification parameters of 30 d aged samples

Relaxation branch term	Amplitude A_i/pA	Time constant $\tau_{i/s}$
0	368.1	6.75×10^5
1	2711.0	5.43
2	1963.1	33.15
3	232.2	83.26
4	240.7	206.42
5	100.2	509.364

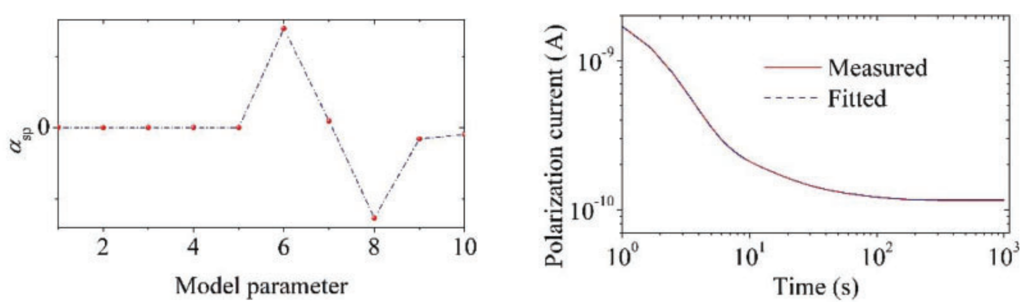

(a) New Cable

Figure 7: (Continued)

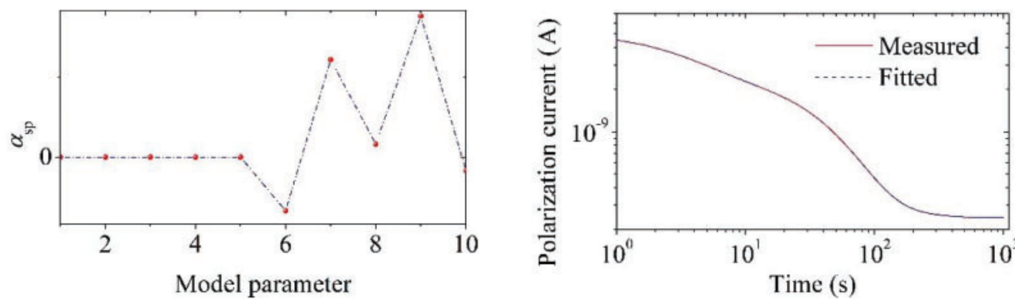

(b) 10 Days Aged Cable

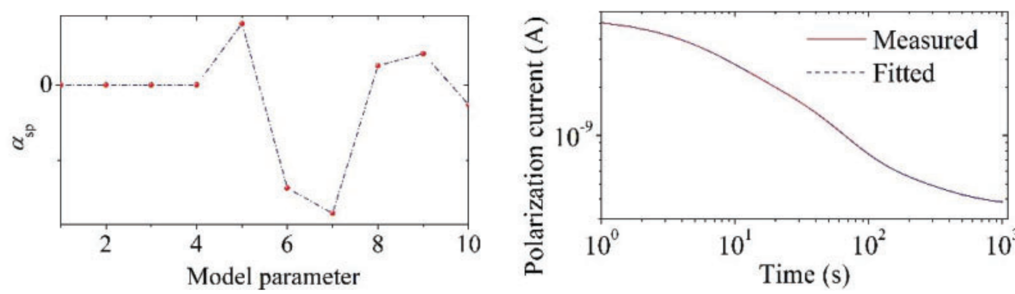

(c) 30 Days Aged Cable

Figure 7: Polarization current and amplitude vector value of cable samples with different insulation states

Fig. 8 shows the first, second and third differential spectral lines constructed by using the simulated polarization current obtained from the SPDMD identification. For the PDC current curve measured by the actual cable sample, it is difficult to distinguish the position of the relaxation peak by the first differential method. Although the second and third differential methods can make the peak stand out, only three relaxation peaks can be identified at most. There is an obvious discrepancy with the actual situation, which further demonstrates the excellent performance of the SPDMD method for parameter identification of the measured XLPE cable.

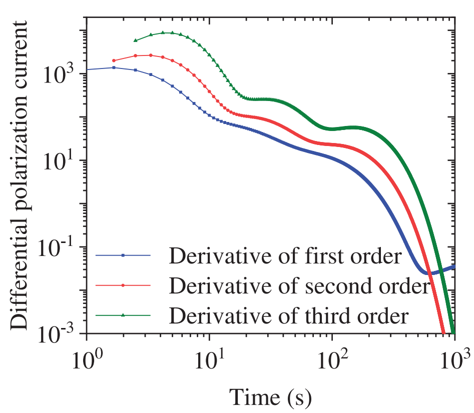

(a) New Cable

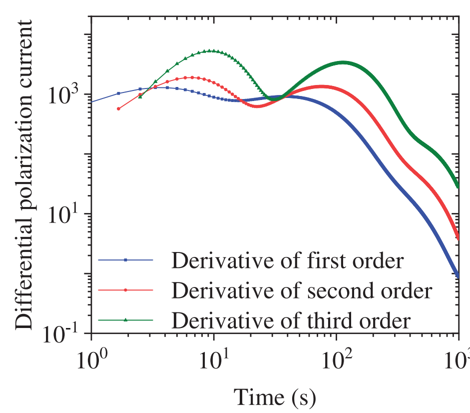

(b) 15 Days Aged Cable

Figure 8: (Continued)

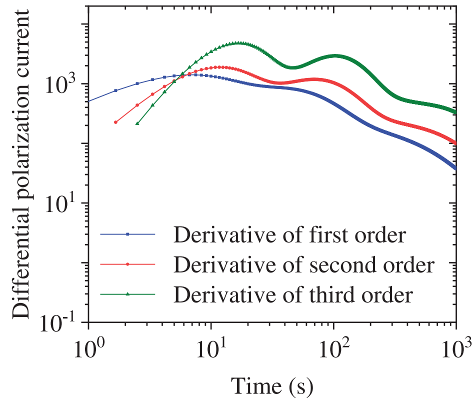

(c) 30 Days Aged Cable

Figure 8: Time-domain differential spectral lines of cables with different insulation states

5.2 Insulation Condition Assessment of Cables Based on SPDMD Results

It is one of the most effective analysis methods for PDC at present to transform the time domain test results of PDC into the frequency domain expression, to obtain the dielectric loss factor spectrum of the insulation, and to diagnose the insulation condition [11]. The complex capacitance of an insulating dielectric can be expressed in terms of the extended Debye equivalent circuit element parameters as follows:

$$C'(\omega) = C_0 + \sum_{i=1}^{n} \frac{C_i}{1 + (\omega R_i C_i)^2} \tag{19}$$

$$C''(\omega) = \frac{1}{\omega R_0} + \sum_{i=1}^{n} \frac{\omega R_i C_i^2}{1 + (\omega R_i C_i)^2} \tag{20}$$

The dielectric loss factor is then

$$\tan\delta(\omega) = \frac{C''(\omega)}{C'(\omega)} \tag{21}$$

Fig. 9 shows the calculated dielectric loss factor spectra of the cable samples at different thermal aging stages. According to the PDC test settings in the previous experiment, the frequency domain range of the dielectric loss factor spectra in this section is 10^{-3} Hz–0.6 Hz. Studies have shown [21] that in the low-frequency range, the parameters obtained by converting the PDC test results to the frequency domain are in good agreement with the direct test results of actual frequency domain measurement methods (such as frequency domain dielectric spectroscopy). It can be seen from Fig. 9 that the dielectric loss factor of the cable after aging increases significantly. References [22] and [23] both showed that the integral $S_{\tan\delta}$ of dielectric loss factor with respect to frequency can be used as a characteristic parameter for effectively evaluating the aging condition of the insulation,

$$S_{\tan\delta} = \int \tan\delta(\omega)\mathrm{d}\omega \tag{22}$$

Afterwards, the relationship between $S_{\tan\delta}$ and the thermal-aging time of the cables is drawn in Fig. 10. It can be seen that $S_{\tan\delta}$ can effectively reflect the insulation condition of XLPE cable.

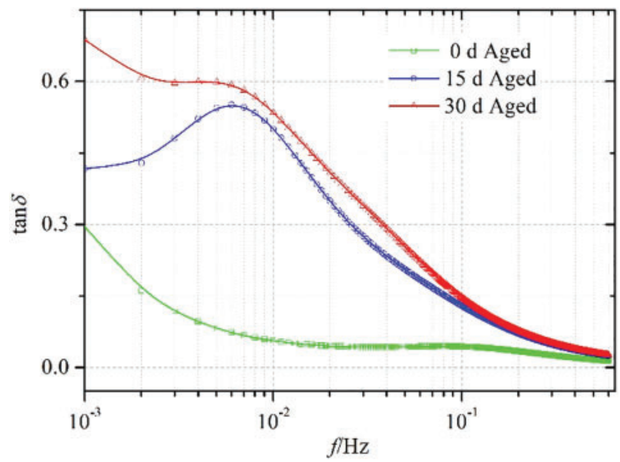

Figure 9: Loss factor spectrum of cables with different insulation conditions

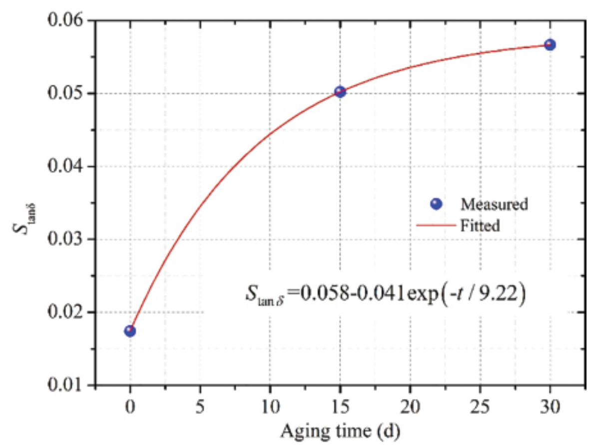

Figure 10: Characteristic parameter $S_{\tan\delta}$ of different aging time

6 Conclusion

This study introduces the sparsity-promoting dynamic mode decomposition algorithm, to identify the equivalent circuit parameters of the extended Debye model. Conclusions are drawn as follows:

i. The number of branches of the extended Debye model can be obtained by calculating the number of non-zero elements in the amplitude vector α_{sp}, and the circuit parameters can be effectively solved thereafter. The simulation and experimental results show that the method can effectively avoid the problems of the traditional differential method in branch identification, such as the unobvious relaxation peak.

ii. For the measured PDC data, the polarization current is less affected by the measurement noise than the depolarization current, which makes the SPDMD identification result based on the polarization current spectral line being better to reflect the response characteristics of the dielectric.

iii. Based on the circuit parameters of the extended Debye model, the time domain PDC test results can be converted into the frequency domain results, and then used to obtain the dielectric loss factor spectrum of the insulation. The integral of the dielectric loss factor on frequency domain can effectively evaluate the insulation condition of the XLPE cable.

Acknowledgement: The authors would like to express their gratitude to the reviewers and the editor.

Funding Statement: This work is supported by the Science and Technology Project of Guizhou Power Grid Co., Ltd. (No. GZKJXM20210405).

Author Contributions: The authors confirm contribution to the paper as follows: study conception and design: W. Wang, M. Chen; data collection: H. Yin; analysis and interpretation of results: W. Wang, Y. Li; draft manuscript preparation: W. Wang, Y. Li. All authors reviewed the results and approved the final version of the manuscript.

Availability of Data and Materials: The data presented in this study are available on request from the corresponding author.

Conflicts of Interest: The authors declare that they have no conflicts of interest to report regarding the present study.

References

1. Morsalin, S., Sahoo, A., Phung, B. T. (2019). Recovery voltage response of XLPE cables based on polarisation and depolarisation current measurements. *IET Generation, Transmission & Distribution, 13(24),* 5533–5540.
2. Zaengl, W. S. (2003). Applications of dielectric spectroscopy in time and frequency domain for HV power equipment. *IEEE Electrical Insulation Magazine, 19(6),* 9–22.
3. Thabet, A., Fouad, M. (2021). Assessment of dielectric strength and partial discharges patterns in nanocomposites insulation of single-core power cables. *Journal of Advanced Dielectrics, 11(4),* 2150022.
4. Thabet, A., Fouad, M. (2022). Dielectric strength and patterns of partial discharges in nanocomposites insulation of three-core belted power cables. *Transactions on Electrical and Electronic Materials, 23(2),* 136–148.
5. Mohamed, A. T. (2021). *Emerging nanotechnology applications in electrical engineering*. Hershey, Pennsylvania, USA: IGI Global.
6. Saha, T. K., Purkait, P., Muller, F. (2005). Deriving an equivalent circuit of transformers insulation for understanding the dielectric response measurements. *IEEE Transactions on Power Delivery, 20(1),* 149–157.
7. Morsalin, S., Phung, B. T. (2019). Modeling of dielectric dissipation factor measurement for XLPE cable based on Davidson-Cole model. *IEEE Transactions on Dielectrics and Electrical Insulation, 26(3),* 1018–1026.
8. Wang, D. Y., Zhou, L. J., Yang, Z. X., Cui, Y., Jiang, J. et al. (2020). A new testing method for the dielectric response of oil-immersed transformer. *IEEE Transactions on Industrial Electronics, 67(12),* 10833–10843.
9. Liu, J. F., Zhang, Y. Y., Xu, J. J., Rui, J., Zhang, G. J. et al. (2017). Quantitative relationship between aging condition of transformer oil-paper insulation and large time constant of extend Debye model. *Electric Power Automation Equipment, 37(3),* 197–202.
10. Liao, W., Zhou, L. J., Li, Z. X., Wang, D. Y., Zhang, J. et al. (2021). An IGBA algorithm based curve reconstruction method of frequency-domain dielectric spectroscopy for OIP bushing with non-uniform moisture distribution. *IEEE Transactions on Transportation Electrification, 7(4),* 3194–3203.

11. Morsalin, S., Phung, B. T. (2020). Dielectric response study of service-aged XLPE cable based on polarization and depolarization current method. *IEEE Transactions on Dielectrics and Electrical Insulation, 27(1),* 58–66.
12. Tang, M. J., Lei, M., Bai, F., Wei, J. L., Xu, H. et al. (2014). Parameter identification based on vector fitting method for extended Debye model of oil-paper insulation system. *High Voltage Engineering, 40(2),* 548–556.
13. Rao, X. J., Zhou, K., Xie, M., Li, M. Z., Xi, H. (2020). Application of stabilization diagram method for solving polarization equivalent circuit parameters. *Transactions of China Electrotechnical Society, 35(10),* 2248–2256.
14. Banerjee, C. M., Baral, A., Chakravorti, S. (2020). De-trapped charge-affected depolarization-current estimation using short-duration dielectric response for diagnosis of transformer insulation. *IEEE Transactions on Instrumentation and Measurement, 69(10),* 7695–7702.
15. Dey, D., Chatterjee, B., Chakravorti, S., Munshi, S. (2010). Importance of denoising in dielectric response measurements of transformer insulation: An uncertainty analysis-based approach. *Measurement, 43(1),* 54–66.
16. Gao, Y. F., Liang, X. D., Chalashkanov, N. M., Wu, C., Dissado, L. A. (2018). Application and significance of the equivalent circuit method in the analysis of dielectric response. *Proceedings of the CSEE, 38(1),* 300–308+368.
17. Qi, J., Jiang, Q. Y., Cao, Y. J. (2008). A general prony identification algorithm for power system transfer function. *Proceedings of the CSEE, 28(1),* 41–46.
18. He, C. B., Li, H. K., Zhao, X. W., Wang, W. M., Wu, S. M. (2019). Analysis method for under-sampled blade tip-timing signal based on the rotational invariance technique with total least squares principle. *Journal of Mechanical Engineering, 55(19),* 103–111.
19. Mihailo, R. J., Schmid, P. J., Nichols, J. W. (2014). Sparsity-promoting dynamic mode decomposition. *Physics of Fluids, 26(2),* 024103–024124.
20. Zhao, A. X., Chen, X., Xu, L., Li, J. M., Deng, J. B. et al. (2020). Application of dielectric response in diagnoses of time and frequency domain on XLPE cable insulation. *High Voltage Engineering, 46(1),* 292–302.
21. Deng, Y. X., Yang, L. J., Guo, X. J., Nie, W., Liao, R. J. et al. (2020). Nonlinear dielectric response characteristics of damp oil-paper insulation and application of H-W model in time-frequency conversion. *IEEE Transactions on Dielectrics and Electrical Insulation, 27(6),* 2078–2086.
22. Du, L., Tan, J. Y., Wu, X. G., Wang, D. S., Chen, X. X. (2020). Study on accelerated electrical aging frequency domain feature of ZnO valve based on extended Debye model. *High Voltage Engineering, 46(5),* 1759–1767.
23. Wu, G. N., Xia, G. Q., Su, M., Zhu, H., Yang, F. B. et al. (2019). Evaluation method for moisture content and aging degree of transformer oil-paper insulation based on frequency dielectric spectroscopy and compensation factor. *High Voltage Engineering, 45(3),* 691–700.